The American Journal of Pathology, Vol. 169, No. 2, August 2006

DOI: 10.2353/ajpath.2006.051041

Tumorigenesis and Neoplastic Progression

Increased Melanoma Growth and Metastasis Spreading in Mice Overexpressing Placenta Growth Factor

Marcella Marcellini,* Naomi De Luca,† Teresa Riccioni,* Alessandro Ciucci,‡ Angela Orecchia,† Pedro Miguel Lacal,§ Federica Ruffini,§ Maurizio Pesce,¶ Francesca Cianfarani,† Giovanna Zambruno,† Augusto Orlandi,‡ and Cristina Maria Failla†

From the Laboratory of Experimental Angiogenesis, Sigma Tau, Rome; the Laboratories of Molecular and Cell Biology† and Molecular Oncology,§ Istituto Dermopatico dell'Immacolata-Istituto di Ricovero e Cura a Carattere Scientifico, Rome; the Anatomic Pathology Institute,‡ Tor Vergata University, Rome; and the Laboratory of Vascular Biology and Gene Therapy,¶ Centro Cardiologico Monzino–Istituto di Ricovero e Cura a Carattere Scientifico, Milan, Italy*

Placenta growth factor (PlGF), a member of the vascular endothelial growth factor family, plays an important role in adult pathological angiogenesis. To further investigate PlGF functions in tumor growth and metastasis formation, we used transgenic mice overexpressing PlGF in the skin under the control of the keratin 14 promoter. These animals showed a hypervascularized phenotype of the skin and increased levels of circulating PlGF with respect to their wild-type littermates. Transgenic mice and controls were inoculated intradermally with B16-BL6 melanoma cells. The tumor growth rate was fivefold increased in transgenic animals compared to wild-type mice, in the presence of a similar percentage of tumor necrotic tissue. Tumor vessel area was increased in transgenic mice as compared to controls. Augmented mobilization of endothelial and hematopoietic stem cells from the bone marrow was observed in transgenic animals, possibly contributing to tumor vascularization. The number and size of pulmonary metastases were significantly higher in transgenic mice compared to wild-type littermates. Finally, PlGF promoted tumor cell invasion of the extracellular matrix and increased the activity of selected matrix metalloproteinases. These findings indicate that PlGF, in addition to enhancing tumor angiogenesis and favoring tumor growth, may directly influence melanoma dissemination. ***(Am J Pathol 2006, 169:643–654; DOI: 10.2353/ajpath.2006.051041)***

Tumor growth and metastasis spreading depend on the formation of new blood vessels that provide oxygen and nutrients.[1] To promote new vessel development, tumor cells secrete angiogenic growth factors that act on the neighboring endothelial cells, inducing proliferation and migration. Recent studies demonstrate that tumor vascularization does not exclusively rely on sprouting of preexisting vessels but also depends on bone marrow-derived progenitor cells.[2]

Among the growth factors implicated in tumor angiogenesis, a major contribution has been ascribed to vascular endothelial growth factor (VEGF).[3] In addition to the proliferative and anti-apoptotic action on endothelial cells, VEGF directly promotes proliferation and/or migration of VEGF receptor-expressing tumor cells.[4–6] VEGF and its receptors are also involved in mobilization of endothelial and hematopoietic stem cells (HSCs) from the bone marrow and their recruitment at the tumor site where they contribute to tumor angiogenesis.[2,7] Although VEGF and its receptor-2 (VEGFR-2) were previously considered major targets for the therapeutic inhibition of angiogenesis, a significant role of VEGF receptor-1 (VEGFR-1) in modulation of angiogenesis has been reported.[8] VEGFR-1 has been shown to be involved in tissue-specific localization and growth of tumor metastases.[9,10] Besides VEGF, other members of the VEGF family, in particular placenta growth factor (PlGF) and VEGF-B, bind to VEGFR-1, but their relative role in VEGFR-1 activation is still undefined.

PlGF plays an important function in adult pathological angiogenesis, whereas it is redundant for the develop-

Supported by the Italian Ministry of Health (grant RF228).

M.M. and N.D.L. contributed equally to this work.

Accepted for publication April 20, 2006.

Address reprint requests to Cristina M. Failla, IDI-IRCCS, Laboratory of Molecular and Cell Biology, Via dei Monti di Creta 104, 00167 Rome, Italy. E-mail: c.failla@idi.it.

ment of the embryonic vasculature.[11] PlGF is chemotactic for monocytes[12] and can restore early and late phases of hematopoiesis after bone marrow suppression through chemotaxis of progenitor cells.[13] PlGF also acts on VEGFR-1-expressing smooth muscle cells and pericytes, thus promoting vessel maturation. In fact, PlGF-deficient mice display less mature vessels compared to wild-type (WT) controls.[11] Besides directly activating its tyrosine kinase receptor, PlGF sustains VEGF activity, probably through increased phosphorylation of VEGFR-2.[14]

Regarding the contribution to tumor angiogenesis, PlGF expression has been detected in human tumor cells both *in vitro* and *in vivo* and is up-regulated during tumor progression.[6,15,16] Moreover, tumor growth and angiogenesis are markedly reduced in PlGF-deficient mice,[11] and overexpression of PlGF in glioma cells leads to increased tumor growth and endothelial cell survival.[17] On the other hand, PlGF could play a negative role in tumor angiogenesis through the formation of PlGF/VEGF heterodimers. These heterodimers are naturally produced by normal and tumor cells in culture,[18–20] binding and activating VEGFR-2, although with reduced affinity compared to VEGF homodimers. Therefore, some authors suggest that the expression of PlGF in tumor tissue could result in inhibition of VEGF-mediated tumor angiogenesis because of the augmented formation of less active PlGF/VEGF heterodimers and the depletion of VEGF homodimers.[21]

We have previously shown that PlGF overexpression in the skin, under the control of a keratin 14 promoter cassette (K14-PlGF mice), results in a substantial increase in number, branching, and size of dermal blood vessels.[22] Mature smooth muscle-coated vessels are abundant in the K14-PlGF mice. High levels of PlGF homodimers are produced by keratinocytes of transgenic mice whereas homodimeric VEGF is significantly reduced compared with control littermates. Therefore, this murine model represents a valuable tool to investigate the effect of PlGF in the biology of tumor growth and tumor-host interactions.

In this study, we injected syngeneic murine melanoma cells in K14-PlGF transgenic mice and matched controls. Using this approach, we could demonstrate that PlGF transgenic animals substantially differ from WT littermates in melanoma growth rate, tumor vascularization, and metastasis formation.

Materials and Methods

Cell Culture and Growth Factors

B16-BL6 murine melanoma cell line was maintained in Dulbecco's modified Eagle's medium (Invitrogen, Carlsbad, CA) supplemented with 2 mmol/L glutamine, 10% fetal calf serum (Hyclone Laboratories, Logan, UT), and antibiotics. Human umbilical vein endothelial cells (HUVECs) were isolated from freshly delivered umbilical cords as previously described[23] and cultured in Endothelial Cell Growth Medium-2 kit from Clonetics (BioWhittaker Inc., Walkersville, MD). The human melanoma cell line M14[6] was maintained in RPMI 1640 medium supplemented with glutamine, fetal calf serum, and antibiotics as described for the B16-BL6 cells. Human fibroblasts were isolated as previously described[24] and cultured in Dulbecco's modified Eagle's medium. The human fibroblast-conditioned medium was obtained from subconfluent cultures incubated for 24 hours in medium without serum, supplemented with 0.1% bovine serum albumin. Recombinant mouse PlGF-2 (rmPlGF) and VEGF (rmVEGF) were purchased from R&D Systems (Minneapolis, MN).

Mice

Transgenic lines were established on a B6D2F1 background as previously described.[22] All mice were treated in accordance with the institutional guidelines for the care of experimental animals. For tumor implantation, mice were anesthetized by intraperitoneal injection of 15 μl/g 2.5% 2,2,2-tribromoethyl alcohol (Sigma-Aldrich, Milwaukee, WI). B16-BL6 cells (1×10^6) in 50 μl of Ca^{2+}/Mg^{2+}-free Hanks' balanced salt solution (ICN Biomedicals Inc., Aurora, OH) were inoculated intradermally in the right flanks of mice by using a 100-μl Hamilton syringe. Tumor attachment rate was 100%; tumor growth was followed daily and measured by a digital caliper. Tumor volume (V) was calculated as $V = \pi/6xab^2$, where a is the longer and b is the shorter of two perpendicular tumor diameters. Mice were sacrificed 25 days after cell inoculation. Animals were necropsied, and organs were examined for the presence of macroscopic metastases. Tumors and lungs were then processed for histological analysis. For lung colonization assay, 1.5×10^4 B16-BL6 cells in 100 μl of Hanks' balanced salt solution were injected into the lateral tail vein. The animals were sacrificed 15 days after inoculation. The lungs were removed and processed for histological analysis.

Histology and Immunohistochemistry

Four-μm-thick paraformaldehyde-fixed, paraffin-embedded tumor or lung sections were used, and specimens were deparaffinized, rehydrated, and processed as previously described.[20] Hematoxylin and eosin (H&E) staining was performed by standard procedures. The antibodies used for blood vessel immunohistochemistry were an anti-mouse PECAM/CD31 polyclonal antibody (M-20; Santa Cruz Biotechnology, Santa Cruz, CA) used at a concentration of 2 μg/ml for 2 hours at 37°C and an anti-α-smooth muscle actin (α-SMA) monoclonal antibody (clone 144, Sigma-Aldrich) diluted 1:30, for 1 hour at room temperature. Negative controls were done by omitting the primary antibody. To detect SDF-1 in tumor sections, the polyclonal antibody (no. 22140192 APX; ImmunoKontact, Oxon, UK) was diluted 1:250 and incubated overnight at room temperature. The signal was amplified with the TSA biotin system (Perkin-Elmer Life Science, Boston, MA) following the manufacturer's instructions.

Morphometric and Statistical Analysis

Necrosis, total tumor area, and number of lung metastases were measured on serial H&E-stained sections at ×20 magnification using a Hamamatsu camera connected to a Nikon microscope and analyzed by Scion Image software (Scion Corp., Frederick, MD). CD31- and α-SMA-stained tumor and lung sections were evaluated with the AxioCam digital camera attached to the Axioplan 2 microscope (Carl Zeiss AG, Oberkochen, Germany). Calibration of each image and the number and area of blood vessels in the tumor stroma (tumor interior, distant from normal tissue more than 100 μm, ×200 magnification), in the tumor periphery (tumor area less than 100 μm distant from the interface with normal tissue, ×400 magnification), in the normal tissue/tumor interface (normal tissue comprised within 100 μm from the tumor edge, ×400 magnification), and in the pulmonary tissue (×200 magnification) were calculated using the KS300, version 3.0 software (Carl Zeiss AG). Quantification was performed on 10 fields per animal by two independent observers. For tumor section analysis, necrosis and hemorrhage areas were excluded. Results are presented as mean ± SEM. Values were evaluated by the nonparametric Mann-Whitney test; $P \leq 0.05$ was considered significant.

Western Blotting Analysis

B16-BL6 melanoma cells in culture were maintained in basal medium containing 0.1% bovine serum albumin for 18 hours and then treated with 100 ng/ml of rmPlGF for 4, 12, and 24 hours. Cell pellets were resuspended in hypotonic buffer (10 mmol/L Tris-HCl, 1 mmol/L ethylenediaminetetraacetic acid, pH 7.4, with protease inhibitor cocktail tablets; Complete, Roche Diagnostics, Basel, Switzerland). An aliquot of extract was saved for determination of protein concentration and the remainder was boiled in the sodium dodecyl sulfate loading buffer. Eighty μg of protein per sample were separated by 6% gel electrophoresis and transferred to a nitrocellulose filter (Amersham Life Science, Buckinghamshire, UK). Protein detection was performed by using a polyclonal antibody against VEGFR-1 (C17, Santa Cruz Biotechnology) that recognizes both the murine and the human form of the receptor, at a concentration of 2 μg/ml, and with a monoclonal antibody against β-actin diluted 1:1000 (AC-40, Sigma-Aldrich). Detection was performed through a chemiluminescence assay (ECL; Amersham Life Science).

Proliferation Assay

B16-BL6 cells and HUVECs were seeded in 96-well tissue culture dishes at a density of 3×10^3 and 5×10^3cells/well, respectively, in the presence of complete medium. After 24 hours, culture medium was substituted with serum-free medium containing 10, 50, and 100 ng/ml of rmPlGF alone or in combination with 10 ng/ml of rmVEGF. The growth factors were then added every 24 hours. Three days later, the plates were stained with rhodamine B as described[25] and the absorbance read at 540 nm in a spectrophotometer (Victor; EG&G Wallac, Turku, Finland). Statistical analysis was performed by the unpaired Student's *t*-test; $P \leq 0.05$ was considered significant.

Peripheral Blood Analysis

Blood was collected and white blood cell counts determined by using a hemocytometer. Plasma samples were obtained and murine PlGF, stem cell factor (SCF), and CXCL12/stromal cell-derived factor 1α (SDF-1α) were measured using the Quantikine Kit ELISA (R&D Systems, Eugene, OR). Peripheral blood mononuclear cells were isolated from heparinized blood after centrifugation over a discontinuous gradient using Lymphoprep (Axis-Shield PoC As, Oslo, Norway). Peripheral blood mononuclear cells (6×10^4) were plated in triplicate in a methylcellulose-based colony assay (StemCell Technologies, Vancouver, Canada) containing interleukin-6 and -3 and SCF. Colonies containing granulocyte/macrophage (CFU-GM), granulocyte (CFU-G), and macrophage cells (CFU-M) were scored after 10 days. Values were evaluated by the nonparametric Mann-Whitney test; $P \leq 0.05$ was considered significant.

Invasion Assay

Eight-μm polycarbonate filters (Nuclepore; Whatman Inc., Clifton, NJ) were coated with 10 μg of Matrigel (BD Biosciences, Bedford, MA). B16-BL6 cells (2×10^5) were introduced in the upper chamber of the Boyden chamber, and graded concentrations of rmPlGF or human fibroblast-conditioned medium were used as stimuli in the lower chamber. After a 3-hour incubation at 37°C, filters were fixed in 4% paraformaldehyde/phosphate-buffered saline and stained in 0.5% crystal violet. Cells from the upper surface were removed by wiping with a cotton swab, and the number of migrating cells attached to the lower surface of the filter was counted in 12 randomly selected microscopic fields (×200 magnification). The invasion index was calculated as the ratio between the number of cells per microscopic field in the experimental condition analyzed and the number of cells per microscopic field in the basal condition (ie, in the absence of any stimulus). Invasion index in the basal condition corresponds to 1. Specificity of rmPlGF-induced stimulation was analyzed by neutralization of the growth factor with a specific antibody (10 μg/ml monoclonal antibody [mAb] 465; R&D Systems) for 45 minutes at room temperature before the invasion test. As a control, an unrelated antibody was used in the same conditions (anti-human VEGF-D mAb 286; R&D Systems). Receptor involvement was analyzed by preincubating the cells with 10 μg/ml of neutralizing polyclonal antibodies anti-mouse VEGFR-1 (AF471; R&D Systems) or anti-mouse VEGFR-2 (AF644; R&D Systems). The invasion assay was performed in the presence of the antibodies. Statistical anal-

ysis was performed by the Student's *t*-test; $P \leq 0.05$ was considered significant.

Reverse Transcriptase and Real-Time Polymerase Chain Reaction (Real-Time PCR)

B16-BL6 melanoma cells in culture were exposed to basal medium containing 0.1% bovine serum albumin for 18 hours and then treated with 100 ng/ml of rmPlGF for 3 hours. Total RNA was prepared using an RNeasy Midi kit (Qiagen, Chatsworth, CA) and reverse-transcribed for 50 minutes at 42°C using an oligo $(dT)_{12\text{-}18}$ primer (Invitrogen) and the Superscript II enzyme (Invitrogen). Quantitative real-time PCR was performed using the SYBR Green PCR core reagent mix (Applied Biosystems, Foster City, CA) and gene-specific primers designed using the Primer Express software (Applied Biosystems). The primers used were: VEGFR-1 forward primer 5′-AGCCTACCTCACCGTGCAAG-3′ and reverse primer 5′-AAAAGAGGGTCGCAGCCAC-3′; MMP1 forward primer 5′-GGAGACCGGCAAAATGTGG-3′ and reverse primer 5′-TGCCCAAGTTGTAGTAGTTTTCCAG-3′; MMP2 forward primer 5′-ATCGCTCAGATCCGTGGTG-3′ and reverse primer 5′-TGTCACGTGGTGTCACTGTCC-3′; MMP3 forward primer 5′-GGGATGATGATGCTGGTATGG-3′ and reverse primer 5′-GCTTCACATCTTTTGCAAGGC-3′; MMP9 forward primer 5′-AAAACCTCCAACCTCACGGA-3′ and reverse primer 5′-GCGGTACAAGTATGCCTCTGC-3′; MMP10 forward primer 5′-GAGAAATGGACACTTGCACCC-3′ and reverse primer 5′-AGGGAGTGGCCAAGTTCATG-3′; MMP13 forward primer 5′-CAAATGGTCCCAAACGAACTTAAC-3′ and reverse primer 5′-CCACTTCAGAATGGGACATATCAG-3′. The reaction conditions were as follows: 2 min-

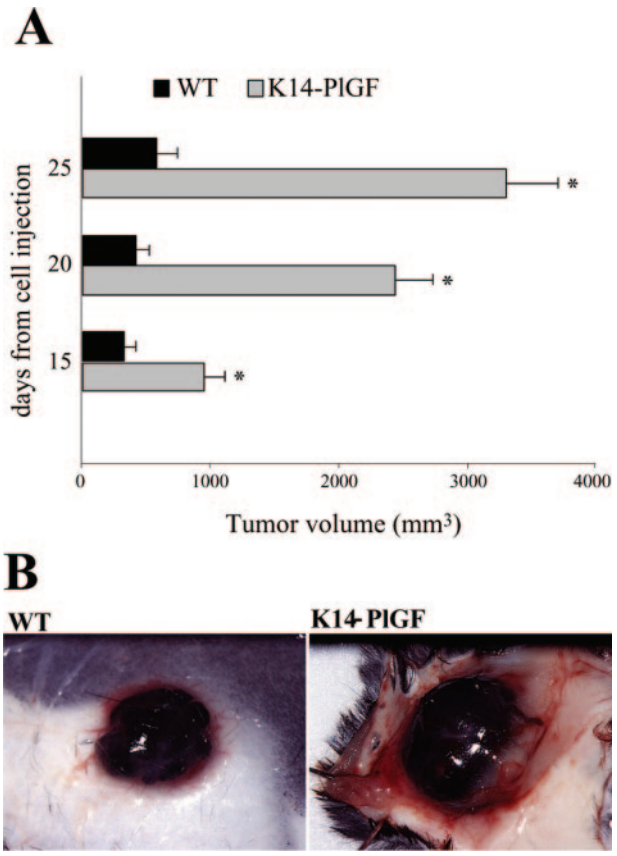

Figure 1. Melanoma cells grow at a higher rate in K14-PlGF transgenic mice. **A:** Tumor volume was measured at different time points after melanoma cell injection in WT and transgenic mice (K14-PlGF). Data were obtained from nine mice per group and were expressed as mean ± SEM. Mann-Whitney's test was used: $^{*}P < 0.001$ versus WT. **B:** Photomicrographs of B16-BL6 melanoma implants of WT and transgenic mice (K14-PlGF) 25 days after tumor injection. An increased number of vessels extending for a large area around the tumor are visible in the transgenic animals.

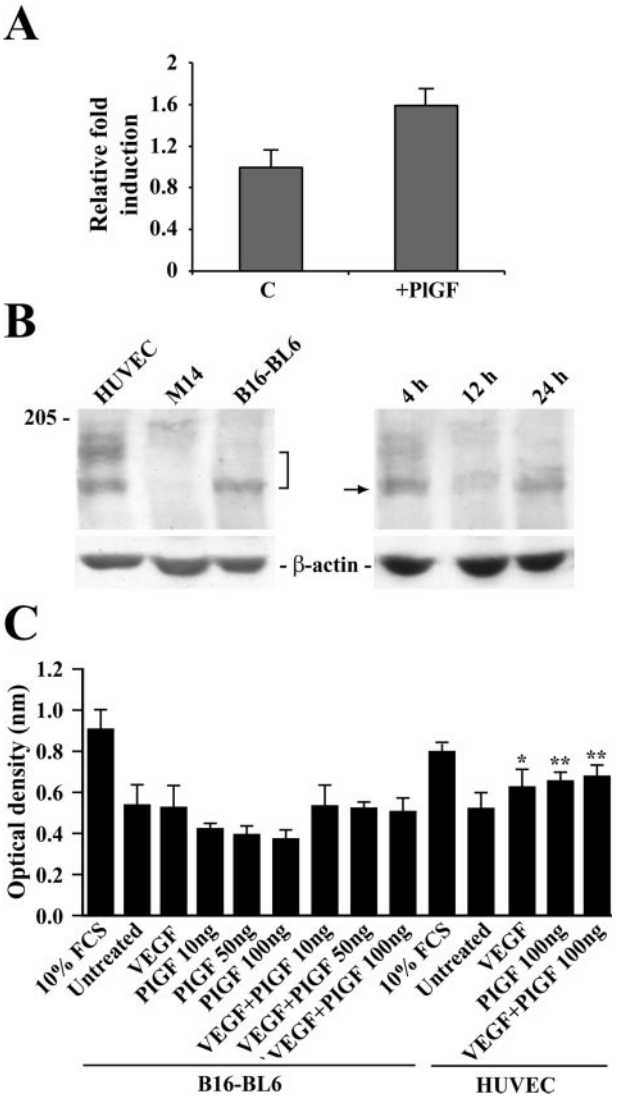

Figure 2. PlGF does not directly promote melanoma cell proliferation. **A:** Reverse transcription and real-time PCR was performed on total RNA extracted from B16-BL6 cells treated or not with rmPlGF for 3 hours. Results are expressed as relative fold induction of the VEGFR-1 mRNA in treated (+PlGF) versus untreated cells (C). **B:** Western blot analysis of cell extracts from B16-BL6 cells, treated or not with rmPlGF for 4, 12, and 24 hours was done by using a polyclonal antibody against the C-terminus of VEGFR-1. **Bar** and **arrow** highlight the VEGFR-1-related signal. HUVECs and M14 cells were used as positive and negative controls, respectively. Molecular weight marker is reported in kd. **C:** B16-BL6 proliferation assay. Cells were incubated with or without the indicated concentrations of rmPlGF in the presence or absence of 10 ng/ml of rmVEGF. HUVECs were used as a positive control in the same proliferation assay. Bars represent the mean of eight replicates ± SEM of a representative experiment. $^{*}P < 0.05$ and $^{**}P < 0.001$ versus untreated cells, unpaired Student's *t*-test.

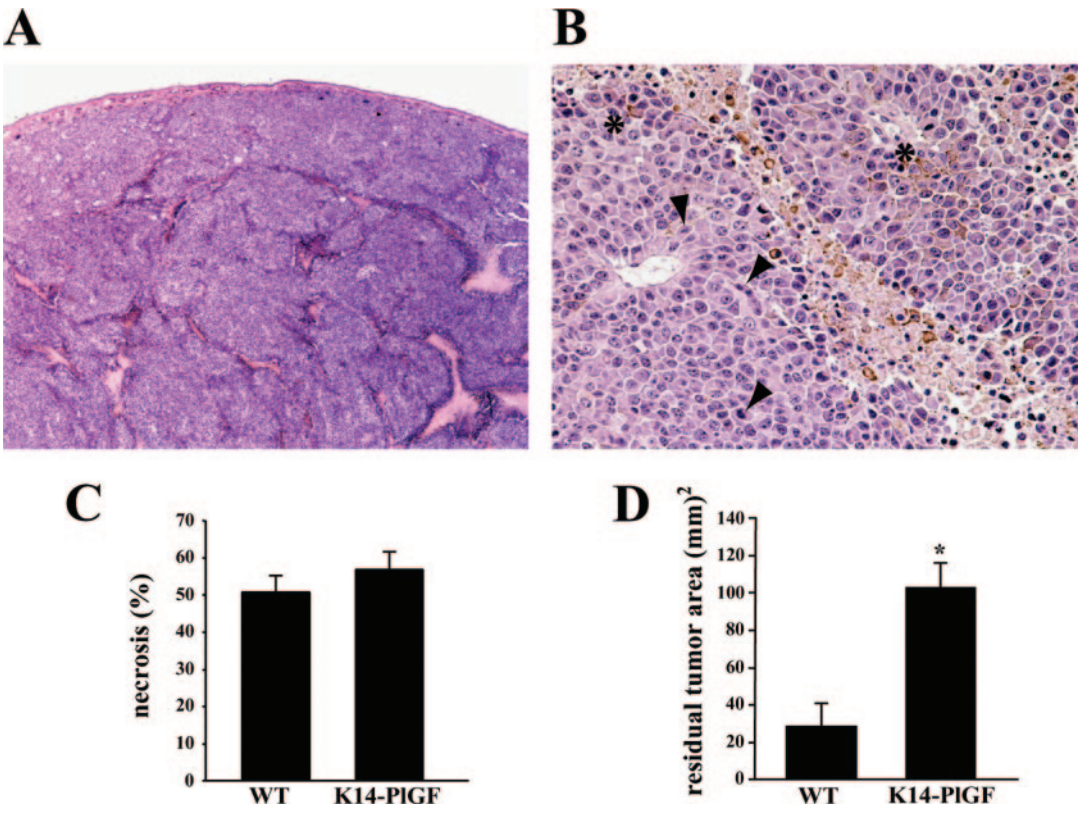

Figure 3. Tumors grown in K14-PlGF transgenic and WT mice display a similar percentage of necrosis. **A:** H&E staining of melanoma cell implant in the transgenic mice. **B:** Higher magnification of the tumor mass showing the intracytoplasmic accumulation of melanin pigment (**asterisks**) and mitotic figures (**arrowheads**). **C** and **D:** Quantitative analysis of the necrosis expressed as a percentage of tumor area (**C**) and of the tumor residual area expressed in mm^2 (**D**). Data were obtained from nine mice per group. Results were expressed as mean ± SEM, $^*P < 0.05$ versus WT, Mann-Whitney's test. Original magnifications: ×20 (**A**); ×400 (**B**).

utes at 50°C (one cycle), 10 minutes at 95°C (one cycle), 15 seconds at 95°C, and 1 minute at 60°C (40 cycles). Gene-specific PCR products were continuously measured by means of the ABI Prism 5700 detection system (Perkin-Elmer, Norwalk, CT) and quantified with a gene-specific standard curve. Value normalization was performed by using a GAPDH standard curve (forward primer 5′-GTATGACTCCACTCACGGCAAA-3′ and reverse primer 5′-TTCCCATTCTCGGCCTTG-3′). Results are expressed as the relative fold increase of the PlGF-stimulated over the control group, which was used as a calibrator.

Zymography

B16-BL6 cells were seeded in 100-mm dishes at a density of 2.5×10^3 cells/cm^2 in the presence of complete medium. After 24 hours, culture medium was substituted with either serum-free alone or serum-free medium containing 20 and 100 ng/ml of PlGF, and cells were maintained at 37°C for a further 24 hours. Conditioned media were collected and concentrated using Centricon YM-10 concentrators (Amicon Bioseparations; Millipore Corp., Bedford, MA). Protein content was determined by the Bradford assay (Bio-Rad, Hercules, CA). Thirty-five-μl aliquots were separated by sodium dodecyl sulfate-polyacrylamide gel electrophoresis in 8% polyacrylamide gels containing 0.1% gelatin under nonreducing conditions, washed first in renaturing buffer (2.7% Triton X-100) and then in a developing buffer (50 mmol/L Tris-HCl, 200 mmol/L NaCl, 10 mmol/L $CaCl_2$, pH 7.5) for 30 minutes, and left in the same buffer overnight at 37°C. Gels were stained with Coomassie brilliant blue R-250 (Bio-Rad) and destained with 5% methanol and 7% acetic acid. A semiquantitative analysis of MMP-2 and MMP-9 activity was performed in triplicate by densitometric methods using Fluor S Max Multi Imager (Bio-Rad), and intensity for each band was expressed as uncalibrated optical density (OD).

Results

Increased Tumor Growth in Mice Overexpressing PlGF

To establish the role of PlGF in promoting tumor growth *in vivo*, B16-BL6 melanoma cells were injected intradermally into the flank of K14-PlGF transgenic mice and WT littermates ($n = 9$). Tumor size was measured daily starting from day 15 after injection, when the tumor mass began to be detectable in both transgenic and control animals. Mice were sacrificed 25 days after cell injection. As shown in Figure 1A, in K14-PlGF mice tumors grew exponentially throughout time with dramatic growth acceleration as compared with tumors in WT animals. A

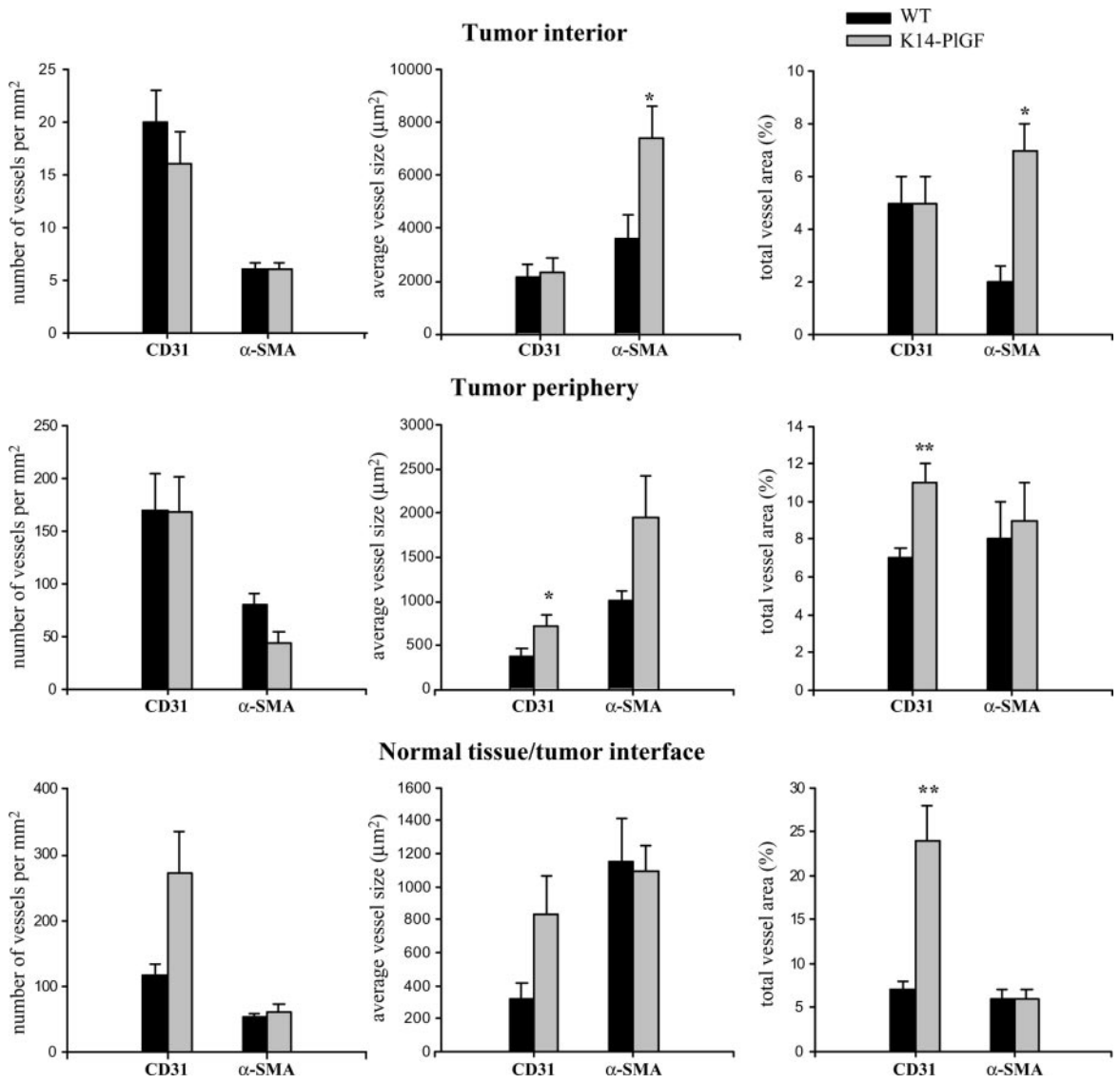

Figure 4. Tumor vessel area is increased in K14-PlGF transgenic with respect to WT mice. Quantitative analysis was performed by immunohistochemical staining of PECAM/CD31- and SMA-expressing vessels. Ten fields per animal were analyzed for each parameter (nine mice per group). Results are expressed as mean ± SEM. Mann-Whitney's test was used: $^{*}P < 0.05$ and $^{**}P < 0.001$ versus WT.

significant difference was already detectable at day 15 after cell injection. At day 25, there was a more than fivefold increase in tumor volume in K14-PlGF mice compared to WT littermates. Macroscopic analysis of tumors dissected from the transgenic animals revealed that the melanoma mass was surrounded by an extended area of prominent vascularization (Figure 1B).

The B16-BL6 cell line showed a constitutive production of PlGF both *in vitro*, as assessed by immunoassay of the culture medium, and *in vivo*, as evaluated by immunohistochemistry. No difference in PlGF expression was observed in tumors grown in transgenic compared to WT mice (data not shown). Thus, to investigate whether the higher amount of PlGF secreted by transgenic mouse keratinocytes could directly stimulate melanoma cell growth, we first analyzed the expression of the PlGF tyrosine kinase receptor VEGFR-1 on B16-BL6 cells. Total RNA was extracted from cells treated or not with 100 ng/ml of rmPlGF for 3 hours, reverse-transcribed, and analyzed by real-time PCR. VEGFR-1 mRNA coding for the transmembrane form of the receptor was detected in melanoma cells and appeared slightly increased on cell stimulation with the growth factor (Figure 2A). At the protein level, VEGFR-1 production was analyzed through Western blotting of B16-BL6 cell extract using an antibody specific for the C-terminal portion of the receptor (Figure 2B). HUVEC extract was used as a positive control and showed two bands corresponding to glycosylated and unglycosylated forms of VEGFR-1.[26] B16-BL6 cells showed only one band that was also observed in human melanoma cells[27] and corresponded to the unglycosylated state. M14 human melanoma cells were used as a negative control because they do not express VEGFR-1.[6] We treated B16-BL6 cells with 100 ng/ml of rmPlGF for 4, 12, and 24 hours, but no significant increase in VEGFR-1 protein expression was observed in

Western blotting analysis (Figure 2B). Then we treated melanoma cells *in vitro* for 3 days with rmPlGF alone or in combination with rmVEGF. None of these stimuli determined an increase in cell proliferation (Figure 2C), indicating that PlGF did not directly influence the growth rate of B16-BL6 cells. HUVECs were used as a positive control in the proliferation assay and significantly responded to either rmPlGF alone (100 ng/ml) or in combination with rmVEGF (10 ng/ml) (Figure 2C) when compared to untreated cells.

PlGF Enhances Peritumoral Vascularization

Microscopically, tumors grown both in transgenic and WT animals appeared as masses of atypical cells located in the dermis and hypodermis. In most cases, the tumor was separated from the overlying epidermis by a thin zone of dermis that appeared highly vascularized (Figure 3A). Occasionally, the skin above the melanoma mass was ulcerated, but ulceration did not correlate with a more aggressive phenotype and subsequent development of metastases. Tumor cells were large with eosinophilic cytoplasm often containing accumulation of melanin pigment and atypical vesicular nuclei with prominent nucleoli. Mitotic figures were frequently observed (Figure 3B). No significant inflammatory infiltrate, in particular macrophages/monocytes, was detected within the lesions. Computer-assisted image analysis of H&E-stained tumor sections was used to measure the amount of necrotic tissue present within the tumor. Despite dramatic acceleration in tumor growth in transgenic mice, a similar percentage of necrosis was observed in tumors of transgenic and WT animals (Figure 3C). Consequently, the area of residual viable tumor was significantly larger in the K14-PlGF compared to WT mice (Figure 3D).

Tumor vascularization was then analyzed by immunohistochemistry using an antibody against the endothelial cell-specific marker PECAM/CD31[28] or an anti-smooth muscle actin (SMA) antibody, which detects both smooth muscle cells and pericytes surrounding endothelial cells.[29] Vessel quantification using the anti-PECAM/CD31 antibody indicated that the relative tumor area occupied by vessels (total vessel area) was similar in transgenic and WT animals in the tumor interior (Figure 4). On the other hand, total vessel area was significantly larger at the tumor periphery (11 ± 1% versus 7 ± 0.5%) in transgenic compared to WT mice, mainly because of the increment in vessel size (721 ± 134 μm^2 versus 382 ± 81 μm^2). Transgenic animals also displayed a marked increase of the vascular area at the interface between normal tissue and tumor (24 ± 4% versus 7 ± 1%), where both vessel density (272 ± 64 vessels/mm^2 versus 117 ± 17 vessels/mm^2) and vessel size (833 ± 235 μm^2 versus 321 ± 96 μm^2) were augmented (Figure 4). Using the anti-SMA antibody, larger vessels (7412 ± 1196 μm^2 versus 3593 ± 897 μm^2), leading to a superior vascular area (7 ± 1% versus 2 ± 0.6%), were detected only in the interior of tumors grown in transgenic mice.

PlGF-Mediated Mobilization of Precursor Cells Might Contribute to Tumor Angiogenesis

In a separate set of experiments we investigated whether the high amount of PlGF normally present in the serum of K14-PlGF mice could promote HSC mobilization from the bone marrow. A colony-forming assay was performed on peripheral blood mononuclear cells obtained from WT and transgenic mice ($n = 10$) and a significantly higher number of colony-forming units could be detected in the K14-PlGF animal-derived samples (Figure 5A).

SCF[13] and SDF-1α[30] are two cytokines implicated in the regulation of HSC trafficking, and we evaluated their amount in plasma samples from transgenic and WT mice ($n = 10$). No significant difference in SCF or SDF-1α plasma levels could be detected between the two animal types (data not shown). SDF-1α was reported to be induced by VEGF and to act by retaining HSCs in close proximity to angiogenic vessels.[7] To investigate whether PlGF could also augment SDF-1α expression *in vivo*, we analyzed tumor sections from transgenic and WT mice. In eight of nine tumors grown in transgenic animals, specific SDF-1α staining was detected in clusters of melanoma cells scattered in the tumor mass (Figure 5B). A similar staining pattern was present in a lower number of tumors from WT mice (five of nine samples).

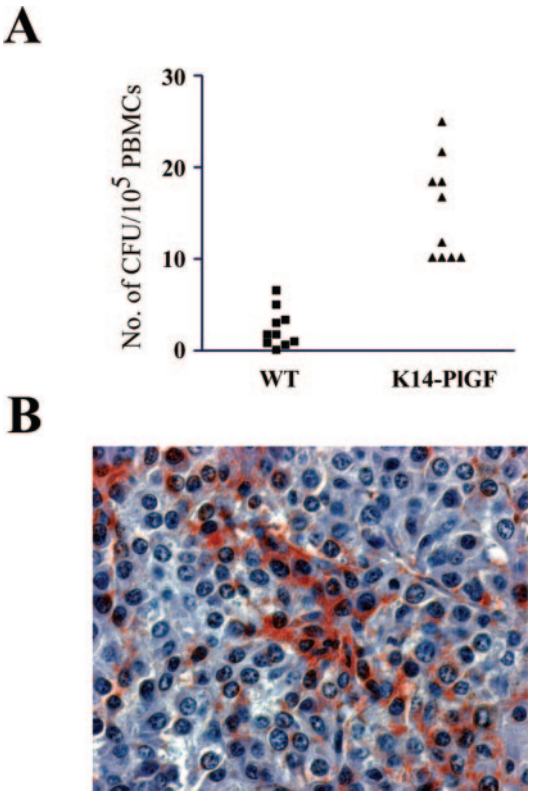

Figure 5. HSC levels are higher in the serum of K14-PlGF transgenic mice. **A:** Methylcellulose-based colony assay of peripheral blood mononuclear cells derived from periphery blood of WT and transgenic (K14-PlGF) mice (10 mice per group). Mann-Whitney's test was used and resulted in a significant difference: $P < 0.001$ transgenic versus WT mice. **B:** Immunohistochemistry for SDF-1α on tumor sections obtained from inoculated animals (nine mice per group). An SDF-1α-specific staining is detected in clusters of melanoma cells inside the tumor mass. Original magnification, ×400.

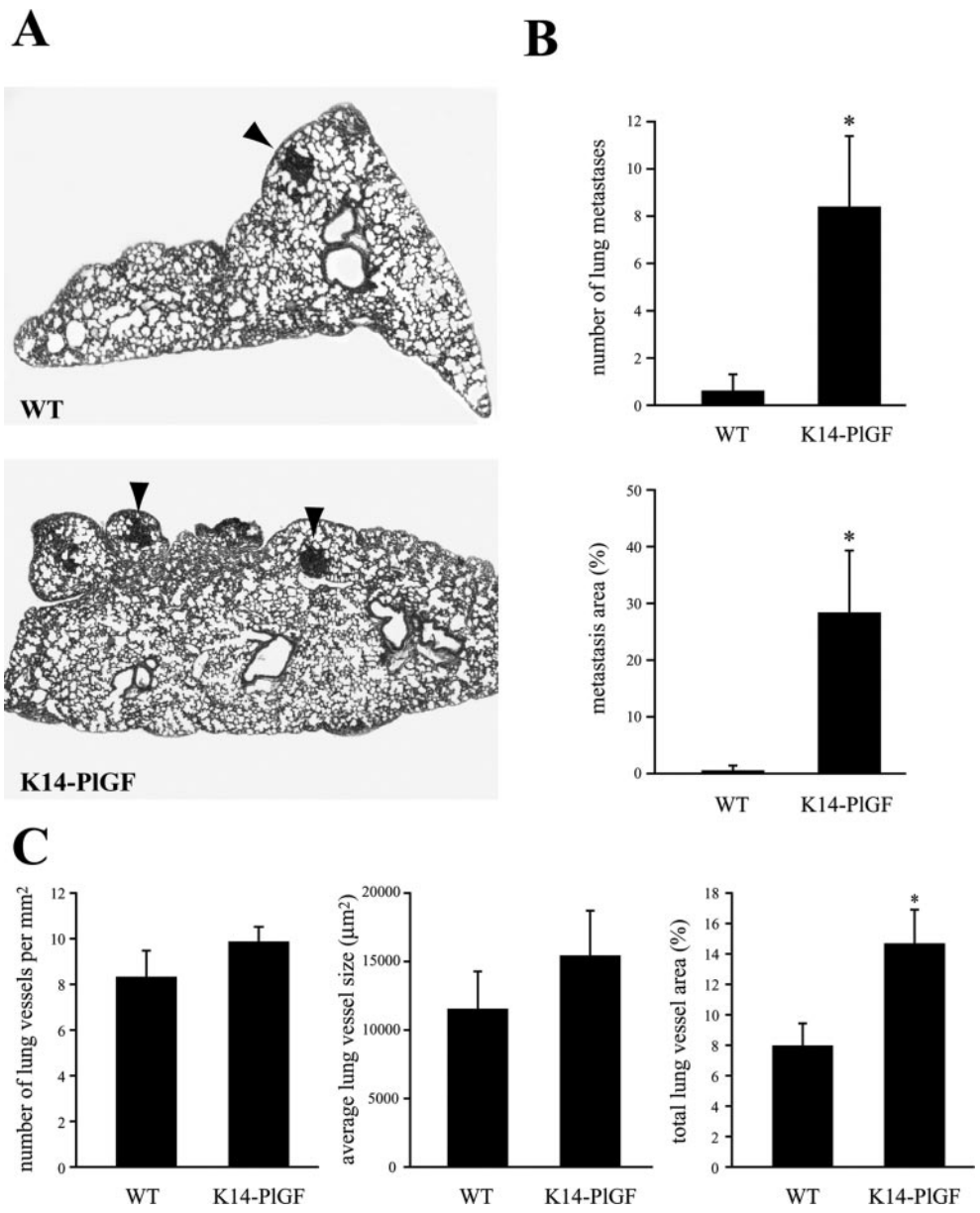

Figure 6. K14-PlGF mice show incremented metastasis spreading. **A:** H&E staining of lung metastatic nodules of WT and transgenic mice (K14-PlGF) 25 days after melanoma cell injection. Original magnifications, ×20. **B:** Number and area of metastases were evaluated by computer-assisted imaging analysis of lung sections in transgenic and WT animals. Data were obtained from nine mice per group. Metastasis area was expressed as percentage of the lung surface. Data were expressed as mean ± SEM, $*P < 0.05$ versus WT, Mann-Whitney's test. **C:** Quantitative analysis of lung vessels in transgenic and WT animals (eight mice per group) by immunohistochemical staining of PECAM/CD31. Ten fields per animal were analyzed. Results were expressed as mean ± SEM, $*P < 0.05$ versus WT, Mann-Whitney's test.

PlGF Leads to Increased Metastatic Spread

Lungs of tumor-bearing mice were macroscopically inspected for the presence of metastatic nodules. Six of nine K14-PlGF mice developed spontaneous pulmonary metastases within 25 days from tumor cell inoculation, whereas metastases were present in only one of nine WT mice. In addition, analysis of lung sections (Figure 6A) showed that the average number and area of lung metastases were significantly higher in K14-PlGF than in control mice (Figure 6B).

The augmented metastatic spreading observed in transgenic animals could be ascribed to increased primary tumor vascularization that facilitates melanoma cell entrance into the blood flow. However, it could be also due to a PlGF-related increment in the number or size of vessels present in distant organs that may favor metastasis colonization. In a separate set of experiments lung sections from transgenic and WT mice ($n = 8$) were analyzed by immunohistochemistry using the anti-PECAM/CD31 antibody and computer-assisted image analysis. A significant enhancement in lung vascularization was observed in transgenic mice compared to WT controls (total vessel area, 14.53 ± 2.27% versus 7.86 ± 1.43%), mainly due to the presence of larger vessels (Figure 6C). To verify whether the in-

creased lung vessel area could facilitate metastasis formation, we induced experimental pulmonary metastases by injecting B16-BL6 melanoma cells intravenously in seven WT and eight transgenic mice. After 2 weeks, metastases were detected in six of eight animals in the transgenic mice group and in one of seven animals in the WT group. Analysis of metastatic foci in the lungs showed that the mean number of metastases in transgenic mice was significantly higher than controls (6 ± 2.07 versus 1 ± 0.87, $P < 0.05$).

PlGF Facilitates B16-BL6 Melanoma Cells Invasion

We then investigated whether PlGF could directly promote B16-BL6 melanoma cell invasiveness. Using a Boyden chamber-based assay, we observed that PlGF supported melanoma cell invasion in a dose-dependent manner (Figure 7A). The specificity of PlGF-induced invasion was confirmed by using a monoclonal antibody against PlGF that significantly inhibited cell migration, whereas an unrelated monoclonal antibody had no effect (Figure 7B). The blocking effect of anti-PlGF antibody was specific, because it had no effect on invasion rate induced by a different stimulus such as human fibroblast-conditioned medium (Figure 7C). Furthermore, treatment of B16-BL6 cells with a polyclonal antibody that selectively blocks VEGFR-1 inhibited cell invasion (Figure 7D) whereas a blocking antibody directed against VEGFR-2 had a modest, although significant, effect (Figure 7D). These data confirmed the involvement of VEGFR-1 in mediating the PlGF effect on B16-BL6 cell invasion.

Tumor invasion requires proteolysis of extracellular matrix mediated by different classes of enzymes. Among them, the matrix metalloproteinase family plays an important role.[31] To investigate the molecular mechanism of PlGF-enhanced melanoma invasion, we treated B16-BL6 cells with 100 ng/ml of rmPlGF for 3 hours, same time of the invasion assay, and analyzed by real-time PCR transcripts coding for matrix metalloproteinases frequently involved in tumorigenesis, such as collagenase 1 and 3 (MMP1, MMP13), stromelysin 1 and 2 (MMP3, MMP10), and gelatinase A and B (MMP2, MMP9). As shown in Figure 8A, the treatment with PlGF did not affect the amount of RNA coding for the two gelatinases, the two collagenases, or the stromelysin MMP-10 but slightly augmented the RNA coding for MMP-3. We also searched for a link between gelatinase activation and constant exposure of melanoma cells to high levels of PlGF in transgenic animals. Gelatin zymography of B16-BL6 cell-conditioned medium (Figure 8B) showed a dose-dependent increase in the release of activated MMP-2 (66 kd) and MMP-9 (86 kd) after a 24-hour stimulation with PlGF (Figure 8, C–D).

Discussion

VEGF is widely recognized as an important regulator of tumor-induced angiogenesis. Nevertheless, some recent

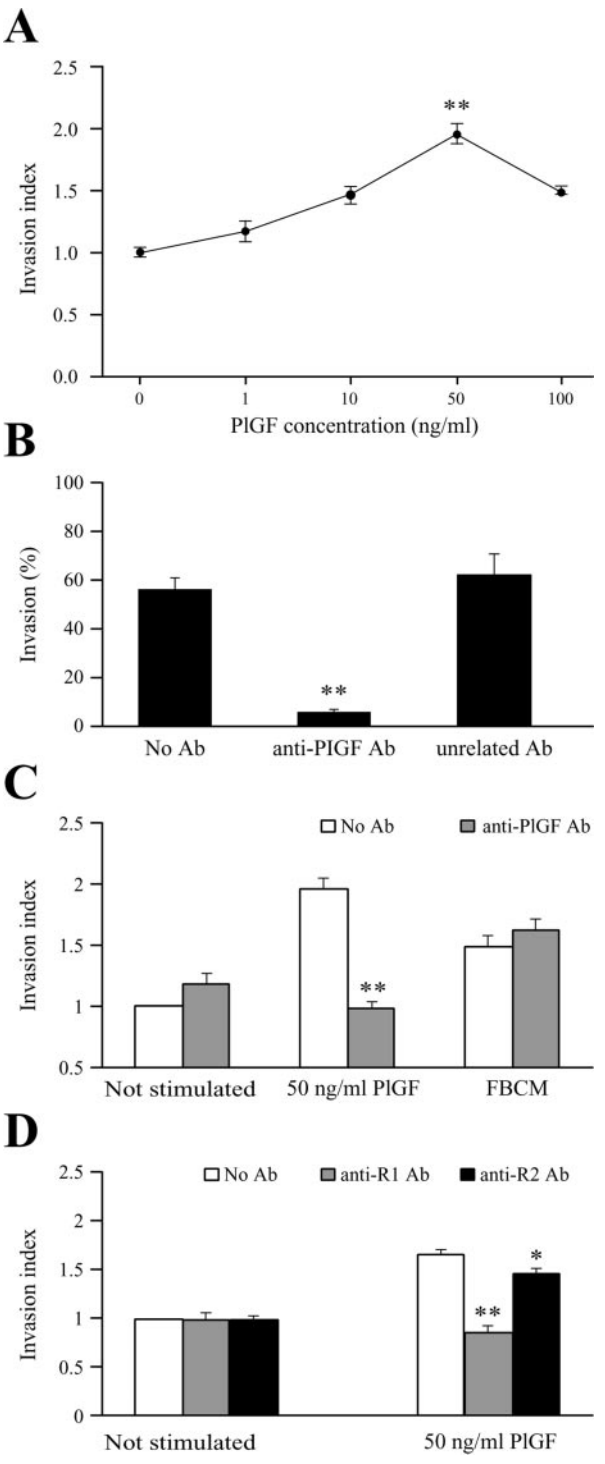

Figure 7. PlGF induces melanoma cell invasion *in vitro*. **A:** B16-BL6 cell capability to respond to rmPlGF was tested in an *in vitro* invasion assay using graded concentrations of the growth factor. $^{**}P < 0.001$ versus basal invasion, two-tailed Student's *t*-test. **B:** B16-BL6 cell invasion of the extracellular matrix in response to 50 ng/ml of rmPlGF was evaluated in the presence of 10 μg/ml of anti-PlGF blocking monoclonal antibody or the same concentration of an unrelated antibody. $^{**}P < 0.001$ versus no Ab, two-tailed Student's *t*-test. **C:** Treatment with an anti-PlGF blocking monoclonal antibody did not affect cell invasion stimulated by another chemotactic stimulus, ie, the conditioned medium of human fibroblasts (FBCM). **D:** Treatment with an anti-mouse VEGFR-1 blocking antibody inhibited PlGF stimulation, whereas anti-mouse VEGFR-2 blocking antibody had a minor but significant effect on PlGF-induced cell invasion. $^{*}P < 0.05$ and $^{**}P < 0.001$ versus no antibody, two-tailed Student's *t*-test. Results represent invasion index or percentage of invasion ± SEM.

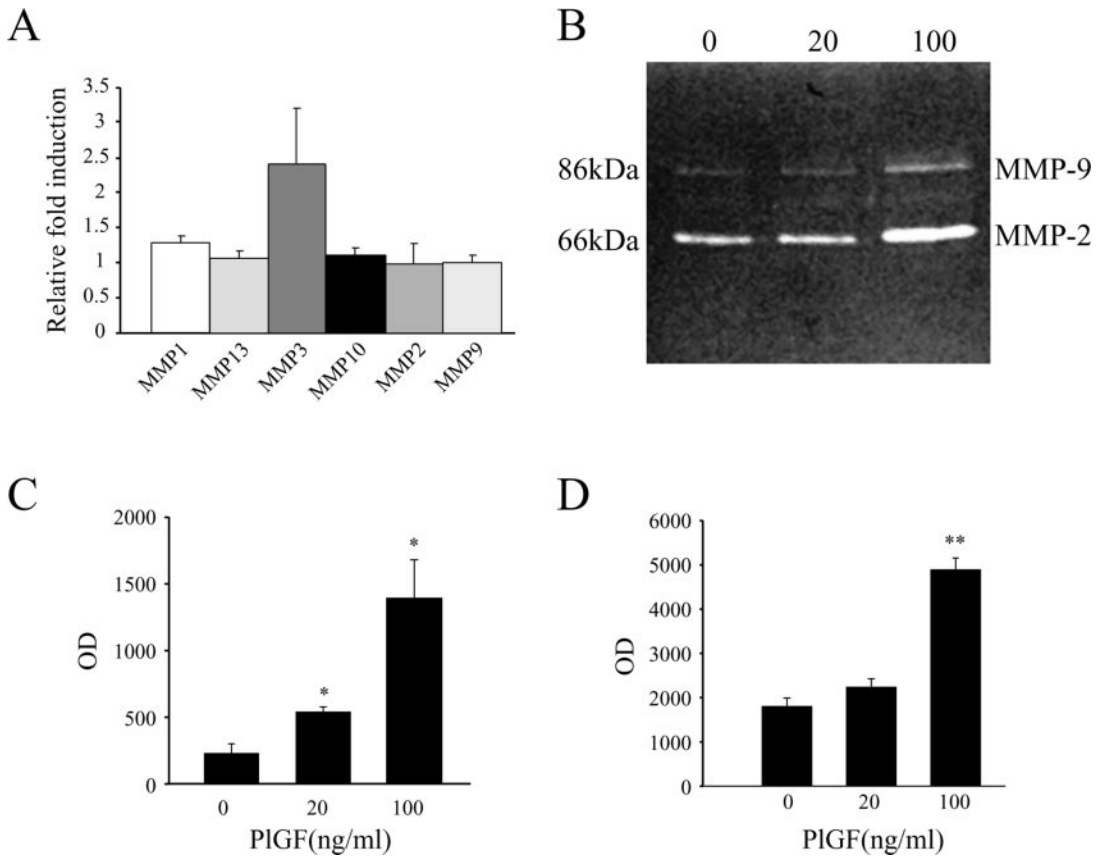

Figure 8. PlGF activates MMP-2 and MMP-9 in a dose-dependent manner. **A:** Reverse transcription and real-time PCR on total RNA extracted from B16-BL6 cells treated with rmPlGF for 3 hours. Amplifications were performed with oligonucleotides specific for the indicated metalloproteinases. Results are expressed as relative fold mRNA induction over that of the untreated cells considered as 1. **B:** Gelatin zymography of conditioned medium from B16-BL6 cells stimulated with the indicated concentration of rmPlGF. **C** and **D:** Densitometric analysis of gelatin zymography of MMP-9 and MMP-2, respectively. Data are expressed as means ± SEM, $^{*}P < 0.02$ and $^{**}P < 0.001$ versus WT, Mann-Whitney's test.

data indicate that additional angiogenic pathways could be involved in tumor angiogenesis and that inhibition of VEGF signaling alone may be insufficient to obtain regression of the disease.[32] In this study, we identify PlGF as an additional factor in tumor angiogenesis and progression. Tumor growth is greatly accelerated in K14-PlGF transgenic mice. Even though B16-BL6 cells do express the PlGF-specific receptor VEGFR-1, they do not proliferate in response to PlGF treatment, and a direct role of PlGF on tumor growth may be excluded. Instead, PlGF favors tumor growth by increasing tumor vascularization. PECAM/CD31-positive vessels at the tumor margin are augmented in number and significantly larger in transgenic mice as compared with WT littermates. These data are consistent with the fact that PlGF overexpression in transgenic animals causes sprouting and increased area of the dermal microvasculature[22] and that treatment with exogenously added PlGF leads to formation of large blood vessels.[33] Interestingly, the number and average size of mature vessels at the tumor periphery, detected with the anti-SMA antibody, do not differ between transgenic and WT animals, even though PlGF was described to promote vessel maturation.[11,22,33] Recently, Taylor and colleagues[34] also reported that PlGF-induced tumor vessels contain less SMA-positive microvessels compared to controls. We could detect an increased number of large and mature vessels only in the interior of tumors developed in K14-PlGF mice. These data support the hypothesis that co-option of pre-existing vessels represents the early stage of tumor growth in highly vascularized tissues[35,36] and that vessels present at the tumor interior are representative of host pre-existing vasculature. During subsequent stages, angiogenesis is initiated at the tumor margin. In our model, the large and mature vessels within the tumor mass are reminiscent of those present in the dermis of K14-PlGF animals,[22] and keratinocyte-produced PlGF later increases peritumoral vascularization but does not sustain maturation of the newly formed vessels.

We could also verify that the high amount of PlGF in the serum of transgenic mice leads to augment circulating HSCs potentially contributing to tumor angiogenesis. These data are in keeping with the previously reported role of PlGF in mobilization of HSCs from the bone marrow.[13,37] PlGF restores the early phase of hematopoiesis after bone marrow suppression through direct chemotaxis of VEGFR-1-positive progenitor cells and the late phase of hematopoietic recovery through MMP-9-mediated release of SCF.[13] In K14-PlGF transgenic animals, we did not observe a significant increment in SCF plasma levels, suggesting that mobilization of HSCs is achieved by direct PlGF-mediated

chemotaxis or through a different SCF-independent mechanism. Growing evidence indicates that SDF-1α is implicated in the regulation of HSC trafficking from the bone marrow to circulation and tissues[38] and in retaining HSCs in close proximity to newly forming vessels where they could produce angiogenic cytokines or directly differentiate into endothelial cells.[7] We could not detect significant differences in the amount of SDF-1α present in plasma samples of WT and transgenic mice. However, a subpopulation of melanoma cells, in particular in transgenic animals, expresses SDF-1α *in vivo* and might contribute in local HSC recruitment. No data are so far available about a direct co-operation between PlGF and SDF-1α in HSC mobilization, but VEGF seems to modulate the mRNA levels of SDF-1α.[7,39] Based on our results, a similar involvement of PlGF may be hypothesized. In this context, PlGF-mediated mobilization of precursor cells together with PlGF induction of SDF-1α expression in the tumor might indirectly contribute to tumor angiogenesis.

Besides affecting tumor growth through local stimulation of angiogenesis, PlGF seems to be involved in metastatic spreading. In our study, the number and area of lung metastases are strongly enhanced in K14-PlGF transgenic animals. PlGF induces a high vascularization of the tumor tissue, thus indirectly facilitating the entrance of melanoma cells into the blood flow and further spreading. We provide evidence that the amount of PlGF present in the blood of transgenic animals is sufficient to augment distal organ vascularization, favoring tissue colonization by metastatic cells. In fact, intravenous inoculation of melanoma cells leads to formation of a greater number of lung metastases in transgenic mice compared to WT littermates. PlGF can also act on VEGFR-1-expressing melanoma cells by increasing their invasion capability. Melanoma cells stimulated *in vitro* with PlGF show a higher mobility rate through the extracellular matrix that is dependent on VEGFR-1 activation because cell treatment with a function-blocking antibody against VEGFR-1 inhibits their migration toward PlGF. An antibody specific for VEGFR-2 had a minor but significant effect on cell invasion, suggesting a contribution of VEGFR-2 signaling pathways, possibly through a mechanism that involves cross talk between the two VEGF receptors.[14] Finally, we demonstrate a consistent increase in secretion of active MMP-2 and MMP-9 after B16-BL6 cell treatment with PlGF. A positive correlation between tumor progression and release of MMP-2 and -9 has been demonstrated in numerous studies,[40–42] and our findings suggest that PlGF could take part in activating specific MMPs.

In conclusion, using a syngeneic animal model of melanoma growth, we characterized the broad role of PlGF in melanoma angiogenesis and progression in an immunocompetent host. Our data indicate that a therapeutic action directed to specific inhibition of PlGF could represent a promising tool to counteract metastatic diffusion of the primary tumor. Moreover, injection of tumor cells in our transgenic mouse model could be a valuable system to test the effects of specific anti-PlGF therapeutic compounds on tumor growth and metastasis formation.

Acknowledgments

We gratefully thank Dr. T. Odorisio for scientific advice; C. Scarponi, D. Rosi, and D. Carlone for skillful technical support; and M. Inzillo for artwork.

References

1. Folkman J: Angiogenesis in cancer, vascular, rheumatoid and other disease. Nat Med 1995, 1:27–31
2. Lyden D, Hattori K, Dias S, Costa C, Blaikie P, Butros L, Chadburn A, Hessing B, Marks W, Witte L, Wu Y, Hicklin D, Zhu Z, Hackett NR, Crystal RG, Moore MAS, Hajjar KA, Manova K, Benezra R, Rafii S: Impaired recruitment of bone-marrow-derived endothelial and hematopoietic precursor cells blocks tumor angiogenesis and growth. Nat Med 2001, 7:1194–1201
3. Neufeld G, Tessler S, Gitay-Goren H, Cohen T, Levi B-Z: Vascular endothelial growth factor and its receptors. Prog Growth Factor Res 1994, 5:89–97
4. Graeven U, Fiedler W, Karpinski S: Melanoma-associated expression of vascular endothelial growth factor and its receptors Flt-1 and KDR. J Cancer Res Clin Oncol 1999, 125:621–629
5. Gitay-Goren H, Halaban R, Neufeld G: Human melanoma cells but not normal melanocytes express vascular endothelial growth factor receptors. Biochem Biophys Res Commun 1993, 190:702–709
6. Lacal P, Failla CM, Pagani E, Odorisio T, Schietroma C, Cianfarani F, Falcinelli S, Zambruno G, D'Atri S: Human melanoma cells secrete and respond to placenta growth factor and vascular endothelial growth factor. J Invest Dermatol 2000, 115:1000–1007
7. Grunewald M, Avraham I, Dor Y, Bachar-Lustig E, Itin A, Yung S, Chimenti S, Landsman L, Abramovitch R, Keshet E: VEGF-induced adult neovascularization: recruitment, retention, and role of accessory cells. Cell 2006, 124:175–189
8. Luttun A, Tjwa M, Moons L, Wu Y, Angelillo-Scherrer A, Liao F, Nagy JA, Hooper A, Priller J, De Klerck B, Compernolle V, Daci E, Bohlen P, Dewerchin M, Herbert J, Fava R, Matthys P, Carmeliet G, Collen D, Dvorak HF, Hicklin DJ, Carmeliet P: Revascularization of ischemic tissues by PlGF treatment, and inhibition of tumor angiogenesis, arthritis and atherosclerosis by anti-Flt-1. Nat Med 2002, 8:831–840
9. Hiratsuka S, Nakamura K, Iwai S, Murakami M, Itoh T, Kijima H, Shipley JM, Senior RM, Shibuya M: MMP9 induction by vascular endothelial growth factor receptor-1 is involved in lung-specific metastasis. Cancer Cell 2002, 2:289–300
10. Kaplan RN, Riba RD, Zacharoulis S, Bramley AH, Vincent L, Costa C, MacDonald DD, Jin DK, Shido K, Kerns SA, Zhu Z, Hicklin D, Wu Y, Port JL, Altorki N, Port ER, Ruggero D, Shmelkov SV, Jensen KK, Rafii S, Lyden D: VEGFR-1-positive haematopoietic bone marrow progenitors initiate the pre-metastatic niche. Nature 2005, 438:820–827
11. Carmeliet P, Moons L, Luttun A, Vincenti V, Compernolle V, De Mol M, Wu Y, Bono F, Devy L, Beck H, Scholz D, Acker T, DiPalma T: Synergism between vascular endothelial growth factor and placental growth factor contributes to angiogenesis and plasma extravasation in pathological conditions. Nat Med 2001, 7:575–583
12. Clauss M, Weich H, Breier G, Knies U, Rockl W, Waltenberger J, Risau W: The vascular endothelial growth factor receptor Flt-1 mediates biological activities. J Biol Chem 1996, 271:17629–17634
13. Hattori K, Heissig B, Wu Y, Dias S, Tejada R, Ferris B, Hicklin DJ, Zhu Z, Bohlen P, Witte L, Hendrikx J, Hackett NR, Crystal RG, Moore MAS, Werb Z, Lyden D, Rafii S: Placental growth factor reconstitutes hematopoiesis by recruiting VEGFR1+ stem cells from bone-marrow microenvironment. Nat Med 2002, 8:841–849
14. Autiero M, Waltenberger J, Communi D, Kranz A, Moons L, Lambrechts D, Kroll J, Plaisance S, De Mol M, Bone F, Kliche S, Fellbrich G, Ballmer-Hofer K, Maglione D, Mayr-Beyrle U, Dewerchin M, Dombrowski S, Stanimirovic D, Van Hummelen P, Dehio C, Hicklin DJ, Persico G, Herbert JM, Communi D, Shibuya M, Collen D, Conway EM, Carmeliet P: Role of PlGF in the intra- and intermolecular cross

talk between the VEGF receptors Flt-1 and Flk-1. Nat Med 2003, 9:936–943
15. Kodama J, Seki N, Tokumo K, Nakanishi Y, Yoshinouchi M, Kudo T: Placenta growth factor is abundantly expressed in human cervical squamous cell carcinoma. Eur J Gynaecol Oncol 1997, 18:508–510
16. Donnini S, Machein MR, Plate KH, Weich HA: Expression and localization of placenta growth factor and PlGF receptors in human meningiomas. J Pathol 1999, 189:66–71
17. Adini A, Kornaga T, Firoozbakht F, Benjamin LE: Placental growth factor is a survival factor for tumor endothelial cells and macrophages. Cancer Res 2002, 62:2749–2752
18. DiSalvo J, Bayne M, Conn G, Kwok P, Trivedi P, Soderman D, Palisi T, Sullivan K, Thomas K: Purification and characterization of a naturally occurring vascular endothelial growth factor/placenta growth factor heterodimer. J Biol Chem 1995, 270:7717–7723
19. Cao Y, Linden P, Shima D, Browne F, Folkman J: In vivo angiogenic activity and hypoxia induction of heterodimers of placenta growth factor/vascular endothelial growth factor. J Clin Invest 1996, 98:2507–2511
20. Failla CM, Odorisio T, Cianfarani F, Schietroma C, Puddu P, Zambruno G: Placenta growth factor is induced in human keratinocytes during wound healing. J Invest Dermatol 2000, 115:388–395
21. Eriksson A, Cao R, Pawliuk R, Berg S, Tsang M, Zhou D, Fleet C, Tritsaris K, Dissing S, Leboulch P, Cao Y: Placenta growth factor-1 antagonizes VEGF-induced angiogenesis and tumor growth by the formation of functionally inactive PlGF-1/VEGF heterodimers. Cancer Cell 2002, 1:99–108
22. Odorisio T, Schietroma C, Zaccaria ML, Cianfarani F, Tiveron C, Tatangelo L, Failla CM, Zambruno G: Mice overexpressing placenta growth factor exhibit increased vascularization and vessel permeability. J Cell Sci 2002, 115:2559–2567
23. Gimbrone MA: Culture of vascular endothelium. Prog Hemost Thromb 1976, 3:1–28
24. Wirtz MK, Glanville RW, Steinmann B, Rao VH, Hollister DW: Ehlers-Danlos syndrome type VIIB. Deletion of 18 amino acids comprising the N-telopeptide region of a pro-alpha 2 (I) chain. J Biol Chem 1987, 262:16376–16385
25. Skehan P, Stoneng R, Scudiero D, Monks A, McMahon J, Vistica D, Warren JT, Bokesch H, Kenney S, Boyd MR: New colorimetric cytotoxicity assay for anticancer-drug screening. J Natl Cancer Inst 1990, 82:1107–1112
26. Orecchia A, Lacal PM, Schietroma C, Morea V, Zambruno G, Failla CM: Vascular endothelial growth factor receptor-1 is deposited in the extracellular matrix by endothelial cells and is a ligand for the $\alpha 5\beta 1$ integrin. J Cell Sci 2003, 116:3479–3489
27. Lacal PM, Ruffini F, Pagani E, D'Atri S: An autocrine loop directed by the vascular endothelial growth factor promoted invasiveness of human melanoma cells. Int J Oncol 2005, 27:1625–1632
28. Dejana E, Corada M, Lampugnani MG: Endothelial cell-to-cell junctions. FASEB J 1995, 9:910–918
29. Valtola R, Salven P, Heikkila P, Taipale J, Joensuu H, Rehn M, Pihlajaniemi T, Weich H, deWaal R, Alitalo K: VEGFR-3 and its ligand VEGF-C are associated with angiogenesis in breast cancer. Am J Pathol 1999, 154:1381–1390
30. Kahn J, Byk T, Jansson-Sjostrad L, Petit I, Shivtiel S, Nagler A, Hardan I, Deutsch V, Gazit Z, Gazit D, Karlsson S, Lapidot T: Overexpression of CXCR4 on human CD34+ progenitors increases their proliferation, migration, and NOD/SCID repopulation. Blood 2004, 103:2942–2949
31. Handsley MM, Edwards DR: Metalloproteinases and their inhibitors in tumor angiogenesis. Int J Cancer 2005, 115:849–860
32. Ferrara N, Gerber H, LeCourter J: The biology of VEGF and its receptors. Nat Med 2003, 9:669–676
33. Nagy JA, Dvorak AM, Dvorak HF: VEGF-A (164/165) and PlGF: roles in angiogenesis and arteriogenesis. Trends Cardiovasc Med 2003, 13:169–175
34. Taylor AP, Rodriguez M, Adams K, Goldenberg DM, Blumenthal RD: Altered tumor vessel maturation and proliferation in placenta growth factor-producing tumors: potential relationship to post-therapy tumor angiogenesis and recurrence. Int J Cancer 2003, 105:158–164
35. Holash J, Maisonpierre PC, Compton D, Boland P, Alexander CR, Zagzag D, Yancopoulos GD, Wiegand SJ: Vessel cooption, regression and growth in tumors mediated by angiopoietins and VEGF. Science 1999, 284:1994–1998
36. Lu W, Schroit AJ: Vascularization of melanoma by mobilization and remodeling of preexisting latent vessels to patency. Cancer Res 2005, 65:913–918
37. Tamarat R, Silvestre J-S, Le Ricousse-Roussanne S, Barateau V, Lecomte-Raclet L, Clergue M, Duriez M, Tobelem G, Lévy BI: Impairment in ischemia-induced neovascularization in diabetes. Am J Pathol 2004, 164:457–466
38. Moore MA, Hattori K, Heissig B, Shieh JH, Dias S, Crystal RG, Rafii S: Mobilization of endothelial and hematopoietic stem and progenitor cells by adenovector-mediated elevation of serum levels of SDF-1, VEGF, and angiopoietin-1. Ann N Y Acad Sci 2001, 938:36–45
39. Hong X, Jiang F, Kalkanis SN, Zhang ZG, Zhang XP, Decarvalho AC, Katakowski M, Bobbitt K, Mikkelsen T, Chopp M: SDF-1 and CXCR4 are up-regulated by VEGF and contribute to glioma cell invasion. Cancer Lett 2006, 236:39–45
40. Itoh T, Tanioka M, Yoshida H, Yoshioka T, Nishimoto H, Itohara S: Reduced angiogenesis and tumor progression in gelatinase A-deficient mice. Cancer Res 1998, 58:1048–1051
41. Huang S, Van Arsdall M, Tedjarati S, McCarty M, Wu W, Langley R, Fidler IJ: Contributions of stromal metalloproteinase-9 to angiogenesis and growth of ovarian carcinoma in mice. J Natl Cancer Inst 2002, 94:1134–1142
42. Hofmann UB, Eggert AAO, Blass K, Brocker E-B, Becker JC: Expression of matrix metalloproteinases in the microenvironment of spontaneous and experimental melanoma metastases reflects the requirements for tumor formation. Cancer Res 2003, 63:8221–8225